



# Study for Appropriate Determination of Sub-working Layer Width Affecting Drilling Performance of a New Sandwich-type Impregnated Diamond Bit in Drilling of Slipping Formation

Il Jin Kim'\*, Yong Nam Kim, Jae Myong Ri, Chol Jong, Kum Hyok Choe

Faculty of Geoscience and Technology, Kim Chaek University of Technology, Pyongyang, 999093 Democratic People's Republic of Korea

\* Corresponding author

DOI: https://dx.doi.org/10.51244/IJRSI.2025.1210000017

Received: 14 September 2025; Accepted: 22 September 2025; Published: 28 October 2025

## **ABSTRACT**

This study aims to analyze the impact of the sub-working layer width on the drilling performance of Sandwich-type Impregnated Diamond Bit (SIDB) in extra-hard, compact and weakly abrasive rock formation called the slipping formation and determine the appropriate sub-working layer width for improving the drilling performance.

In this study, the rock-cutting simulation using Particle Flow Code in Three Dimension (PFC3D) software based on the discrete element method, the field drilling test and the particle-size analysis of the cuttings produced during the drilling were carried out.

The results of the rock-cutting simulation using PFC3D indicate that the distance between two cutters clearly affect the cutting efficiency and the appropriate sub-working layer width for improving the drilling performance is 1.25mm.

For the field drilling test, SIDB of  $\Phi$ 59/41 mm with the sub-working layer width of 1.25mm was manufactured and applied to the quartzite formation of Ongjin mining area. The result of field drilling test shows that the rate of penetration (ROP) and the drilling footage are 1.05m/h and 10.8m, respectively, and are 3-5 times bigger than those of the conventional bit.

The particle-size of the cuttings produced during the drilling ranges from 34.5-108.6 µm, which is much larger than that of the conventional bit. This indicates that the rock-breaking mode is clearly transferred from micro-cutting mode to the combination mode of micro-cutting and volumetric-breaking.

This study has proposed a new design approach to effectively overcome the slipping formation.

**Keywords:** diamond bit, slipping formation, drilling performance, rate of penetration, rock-cutting

## INTRODUCTION

Impregnated diamond (ID) bits are widely used for drilling hard rocks and materials in geological exploration, oil and gas extraction, mining and construction drilling fields [1, 2]. As ID bits are applied to deeper wells, the probability of encountering extra-hard, compact and weakly abrasive rock formation during drilling is increasing. The drilling performance of ID bits in slipping formations is very low, which is largely related to the following three mechanical characteristics of this formation. (1) Relatively high rock hardness (approximately 5000MPa but up to 7000MPa in special formation) due to high quartz content; (2) High rock strength (uniaxial compressive strength of 150MPa or higher) due to composition of very small mineral grains (0.01-0.2mm) and local siliceous cementation; (3) weak abrasiveness [3, 4]: The low abrasiveness of rock formation results in low rate of penetration (ROP) and small rock cuttings. Therefore, the abrasive action of cuttings to the bit matrix is

ISSN No. 2321-2705 | DOI: 10.51244/IJRSI | Volume XII Issue X October 2025



limited, and diamond grains don't easily protrude from the bit matrix [5, 6]. When the conventional diamond bit is used for these rock formation, "Slipping phenomenon" appears and the rate of penetration is very low (generally ranging from 0.2 to 0.3m/h) [7].

In order to improve the ROP of ID bit in slipping formation, many researches are conducted. A researcher proposed a method putting down abrasive material (quartz sand) into the borehole [8]. This method promotes the wear of matrix and protrusion of diamond grains by putting down abrasive material into the borehole, thereby the drilling performance is improved. Other researchers have proposed the grinding of bit bottom surface and acid treatment method [9]. However, the methods mentioned above have a long auxiliary working time and a risk drilling accidents. Due to these limitations, the authors have solved the problem of diamond protrusion and pull out of worn diamond by lowering the wear resistance of the matrix and reducing the retention of the matrix on diamond through matrix formula design [4, 10]. In this method, the surface of diamond grains is coated with WC powder and then mixed with the matrix powders and sintered. However, this method is also advantageous for diamond protrusion, but it has the disadvantage of short lifetime of the bit due to low wear resistance of the bit matrix and low retention of the matrix on diamond. Another study for improving the drilling performance of diamond bit in slipping formation is to change the bottom shape of bit [11]. In other words, they increased the thrust per unit area acting on the bottom of the bit by changing the bottom shape of the bit to the inner protrusion shape, the outer protrusion shape, the central protrusion shape, the cross-section shape and concentric circular shape and improved the drilling efficiency. However, this method also has disadvantage that the bottom surface of bit gradually changes the flat shape as the bit matrix is worn during drilling.

To overcome this shortcoming, a researcher has proposed the SIDB maintaining the concentric circular shape of the bottom surface of bit during drilling and remarkably improved the drilling performance in the slipping formation [12]. The matrix part of SIDB consists of the diamond-containing layers and diamond-free layers toward the radial direction. These layers may be worn at different speeds during drilling due to different wear resistance. That is, the working layers with high wear resistance (diamond-containing layer) are slowly worn and the sub-working layers with low wear resistance (diamond-free layer) are rapidly worn. As a result, a zigzag structure is formed at the bottom surface of bit, which reduces the contact area between the bottom surface of bit and rock formation, the load acting per unit area is increase and the rock breaking is promoted. At the same time, in the borehole bottom, the rock ridges corresponding with the zigzag shape of bit are formed. The increase in the free surface in these rock ridges results in a decrease in rock strength and the rock ridges are easily broken during drilling. As a result, unlike the conventional diamond bit, the rock-breaking process of SIDB is conducted by using the combination mode of micro-cutting and volumetric-breaking, and because the produced rock cuttings is relatively large, it promotes the wear action on the bit matrix and is also favorable for diamond protrusion. The excellent rock-breaking effect of SIDB is greatly influenced by sub-working layer width.

However, further studies are needed to analyze the impact of sub-working layer width on the drilling performance and rock-breaking characteristics of SIDB in slipping formation and to determine the appropriate sub-working layer width for improving the drilling performance.

This study aims to investigate the impact of sub-working layer width on the drilling performance and rock failure characteristics of SIDB in slipping formation and determine the appropriate of the sub-working layer width by using PFC3D-based rock failure simulation, field drilling test and particle-size analysis of cuttings produced. This study has the certain significance in effectively overcoming the slipping formation and improving the drilling performance.

#### **METHODOLOGY**

## **Design and Manufacturing of SIDB**

Design of Sandwich Structure

We have obtained the following common insights from previous researches on the design of diamond bit used for the drilling of the slipping formation [3, 7]. (1) The contact area between the working surface of the bit and the rock should be as small as possible. (2) The self-sharpening of the diamond bit should be ensured. Due to the

ISSN No. 2321-2705 | DOI: 10.51244/IJRSI | Volume XII Issue X October 2025



small particle-size of the cuttings and wear abrasiveness of the rock in the drilling of the slipping formation, the abrasive ability of the cuttings to the matrix should be enhanced by increasing the particle-size of the cuttings and the abrasive resistance of the matrix should be weakened.

To achieve the design purposes, the sandwich-type impregnated diamond (SID) cutter with two sub-working layers and three main working layers was designed. Due to the main working layer and sub-working layer are different in the wear resistance, the flat bottom of SIDB at the beginning gradually changes to a zigzag structure during the drilling process (Fig. 1).

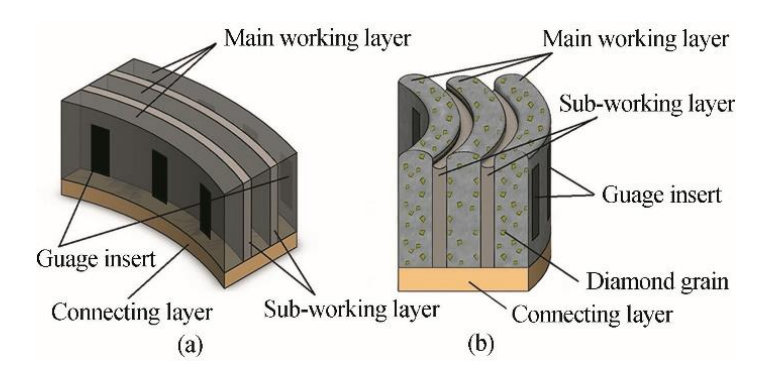


Fig. 1. Structure of SID cutter: before wear (a), after wear (b).

Because the wear resistance of the main working layer and sub-working layer is different, the sandwich-type structure at the bottom surface of matrix is gradually formed during the drilling process. The zigzag structure formed at the bottom surface of the matrix reduces the contact area between the bottom surface of SIDB and the rock, thus creating a favorable condition for drilling. In addition, the zigzag structure at the bottom of SIDB also forms zigzag rock ridges in the bottom of borehole, and the failure of such rock ridges is affected by the sub-working layer width). That is, if the width of the rock ridges is too small, the failure effect of the sandwich structure cannot be fully demonstrated, and if the width of the rock ridges is too large, the rock ridges will not break and rather will act as a hindrance to the drilling. Therefore, the optimum choice of the sandwich parameters can improve the drilling performance and rock-breaking characteristics of SIDB by achieving primary failure (micro-cutting failure) by diamond and secondary failure (volumetric-breaking) by sandwich structure.

#### **Diamond Parameters and Matrix Formula**

The use of diamond grains with high compressive strength and high impact resistance can improve the performance of diamond bit considerably. The diamond concentration in the matrix also has a great impact on the drilling performance of diamond bit. In this study, we used MBD<sub>8</sub> diamond with a particle-size of 60/80 mesh and designed a diamond concentration of 75% in the matrix [13]. The matrix of diamond bit which targets the slipping formation with a very hard, compact and weak abrasive should be designed relatively weak [14]. In particular, the matrix formula design of diamond bit for the slipping formation is one of the most important design factors for realizing self-sharpening of bit and improving life. In general, various metal powders such as tungsten carbide, iron, copper, nickel, cobalt and others are used for the matrix of bit [15, 16]. From previous studies, we designed the hardness of the matrix as HRC 20/25. Table 1 shows the matrix formula design of SIDB for testing.

Table 1. Matrix formula design

Composition	WC	Fe	Cu	Ni	Co	Sn
Content (wt.%)	20	35	25	15	3	2

# **Design of Mold and Brazing Process**

We first prepared cold-pressing compacts of SID cutters. The material of cold-pressing mold is the carbon tool



ISSN No. 2321-2705 | DOI: 10.51244/IJRSI | Volume XII Issue X October 2025

steel. The prepared cold-pressing compacts were sintered using by TLZK2013 vacuum hot-pressure sintering machine. The sintering parameters are shown in Table 2. Fig. 2 shows the structure of graphite mold for sintering the cold-pressing compacts.

Table 2. Sintering parameters for SID cutter

Sintering parameters	Sintering Temperature (°C)	Sintering Pressure (MPa)	Retention time (min)	
Value	930	16	3	

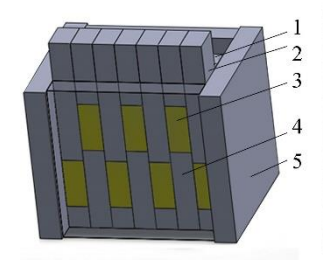




Fig. 2. Structure of graphite mold assembly: separator plate (1), presser (2), cold-pressing compact (3), support (4), side plate(5).

We brazed the SID cutter to bit steel body. The design of brazing steel body and SID cutter is important to maximize brazing strength and to reduce brazing temperature as much as possible. The increase in brazing strength is directly related to the problem for preventing drilling accidents and ensuring the working stability of SIDB. To ensure the stability of SIDB and prevent diamond thermal damage at high temperatures, brazing temperature while ensuring sufficient brazing strength should be lowered as much as possible. We used the silver solder as brazing material based on several experiments. Table 3 shows the composition and melting point of the silver solder materials.

Table 3. Composition and melting point of brazing material

Chemical composition of silver solder material (wt.%)					Melting point (°C)
Ag	Cu	Zn	Ni-Co	Cd	
50	15.5	15.5	3	16	630-680

We reduced the brazing temperature to below 700 °C and prevented the strength reduction of diamond grains generated by thermal shock. A high frequency brazing machine of GP-40 type was used in brazing.

## Simulation of Rock-Cutting Process using PFC3D Software

Particle Flow Code (PFC) based on the discrete element method is widely used to solve rock failure and geotechnical problems [17, 18]. To investigate the impacts of sub-working layer width on the rock-breaking efficiency and characteristics of the sandwich structure, a rock-cutting simulation using PFC3D software was carried out.

#### **Characteristics of Rock Formation**

The hard rock mass of Ongjin mining area is mainly quartzite. Microscopic analysis of rock samples shows that the main mineral is quartz (silica content is more than 98%) with a small amount of muscovite. This rock was formed by the metamorphism of quartz sandstone, which had a granular crystalline structure and a homogeneous texture. The size of the mineral particles ranges from 0.03 to 0.18 mm (Fig. 3).





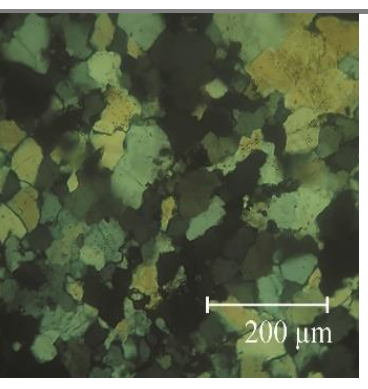


Fig. 3. Photograph (left) and micrograph (right) of the rock sample in Ongjin mining area.

The quartz, which accounts for more than 98% of the minerals forming rock, is a very hard (Mohs Hardness of 7 grade) and compact rock.

To measure the compressive strength and tensile strength of rock sample, the uniaxial compressive tests and Brazilian tensile tests were carried out. The rock samples for strength measurement have a diameter of 31.7 mm and a height of 63.4 mm. To measure the compressive strength and tensile strength of rock sample, a WDW-600 microcontroller electronic universal test device (Chang Chun Science and Technology Testing Instrument Co., LTD, China) was used. The uniaxial compressive strength of rock sample is measured directly, but the tensile strength is calculated indirectly by measuring the value of the maximum compressive force and then using the following equation:

$$\sigma_t = \frac{2P_{\text{max}}}{\pi L D} \tag{1}$$

Where,  $P_{\text{max}}$  is the maximum compressive force obtained from the Brazilian tensile test, L and D is the height and diameter of the rock sample, respectively [19]. The compressive strength and tensile strength of the quartzite sample are 166 MPa and 17.6 MPa, respectively. From the lithological and mechanical characteristics of the rock sample, it is known that the quartzite formation of Ongjin mining area belongs to an extra-hard, compact and weakly abrasive rock formation [20].

Bonded-Particle Model for Rock-Cutting Simulation and Model Calibration

In the PFC, the bonded-particle model reproduces the various failure characteristics of rock such as elasticity, fracture, acoustic emission, damage accumulation, hysteresis and expansion that produce material anisotropy [21]. The bonded-particle mode for rock is represented by a dense packing of spherical particles with non-uniform size interconnected and has the micro-properties such as the stiffness and strength parameters of the particles and the bonds. From a relatively simple set of micro-properties, the bonded-particle model can produce the failure behavior of real rock. Therefore, the important problems in application of the bonded-particle model for rock is that the micro-properties of the model are reasonably chosen so that the rock model can accurately reflect the mechanical properties of the original rock. The important mechanical properties of rock include Young's modulus, Poisson's modulus, compressive strength and tensile strength. These properties are used to calibrate the model's micro-properties. To calibrate the relationship between the mechanical properties of rock samples and the micro-properties of model, a bonded-particle model was created. The model is cylindrical with a diameter of 31.7 mm and a height of 63.4 mm, and consists of 65,534 particles. The rock model created for the simulation also has a porosity of 30%. The uniaxial compressive test and direct tensile test were carried out to obtain the Young's modulus, Poisson's modulus, uniaxial compressive strength, tensile strength and stress-strain curves of rock samples. Table 4 shows the micro-properties used to represent the mechanical properties of the intact rock in the bonded-particle model for PFC3D. The results of the uniaxial compressive test and the direct tensile test are shown in Fig. 4.

Table 4. Micro-properties of the bonded-particle model for PFC3D



Particle	Value	Parallel bond	Value
μ	0.5	$\bar{\mu}$	0.5
R <sub>min</sub> (mm)	0.05	$\overline{E_c}$ (Gpa)	40
$R_{\min}/R_{\max}$	1.66	$\overline{k_n}/\overline{k_s}$	2.5
E <sub>c</sub> (GPa)	65	Pb_ten, (Mpa)	150
$k_{\rm n}/k_{\rm s}$	2.5	Pb_coh (Mpa)	80
$\rho  (\text{kg/m}^3)$	2650	<i>Pb_fa</i> (°)	30

Where  $\mu$  is the frictional coefficient of particles,  $\bar{\mu}$  is the frictional coefficient of contacts,  $\rho$  is the particle density, and  $E_c$  is the Young's modulus at each particle-particle contact,  $R_{\min}$  and  $R_{\max}$  are minimum and maximum radius of particle,  $k_{\text{n}}/k_{\text{s}}$  is the ratio of normal stiffness to shear stiffness of particle,  $Pb\_ten$  and  $Pb\_coh$  are the normal strength and cohesive strength of parallel-bond,  $\overline{E_c}$  is the Young's modulus of each parallel-bond,  $\overline{k_n}/\overline{k_s}$  is the ratio of normal stiffness to shear stiffness at the parallel-bond,  $Pb\_fa$  is friction angle of parallel-bond.

The mechanical properties of the intact rock obtained from uniaxial compressive test and direct tensile test are shown in Table 5

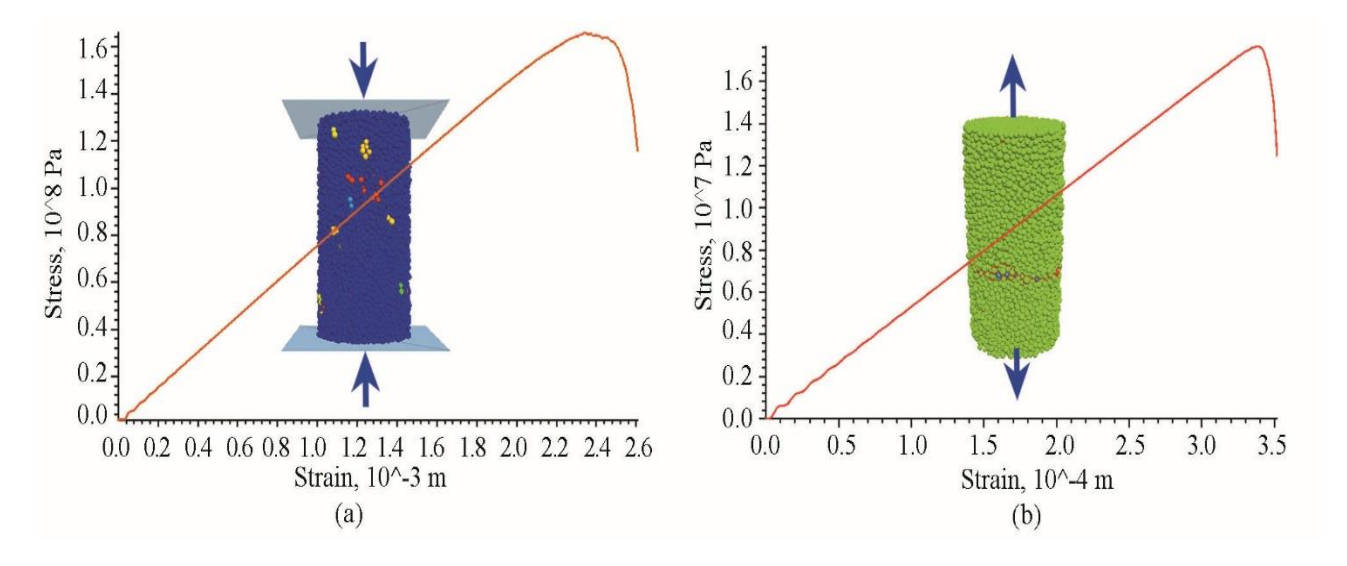


Fig. 4. Result of the uniaxial compressive test (a) and the direct tensile test (b).

Table 5. Mechanical properties of intact rock obtained from tests

E (GPa)	ν	σ <sub>c</sub> (MPa)	σ <sub>t</sub> (MPa)
66.4	0.31	166	17.6

Rock-Cutting Simulation using PFC3D

The rock-cutting simulation tests were conducted to analyze the rock-breaking characteristics of SIDBs with the sub-working layer width of 1, 1.25, 1.5, and 1.75 mm. The cutting depth of diamond grains was 1/10 times of the diameter of diamond grain and the cutting speed was 2 m/s. The simulation results are shown in Fig. 5.



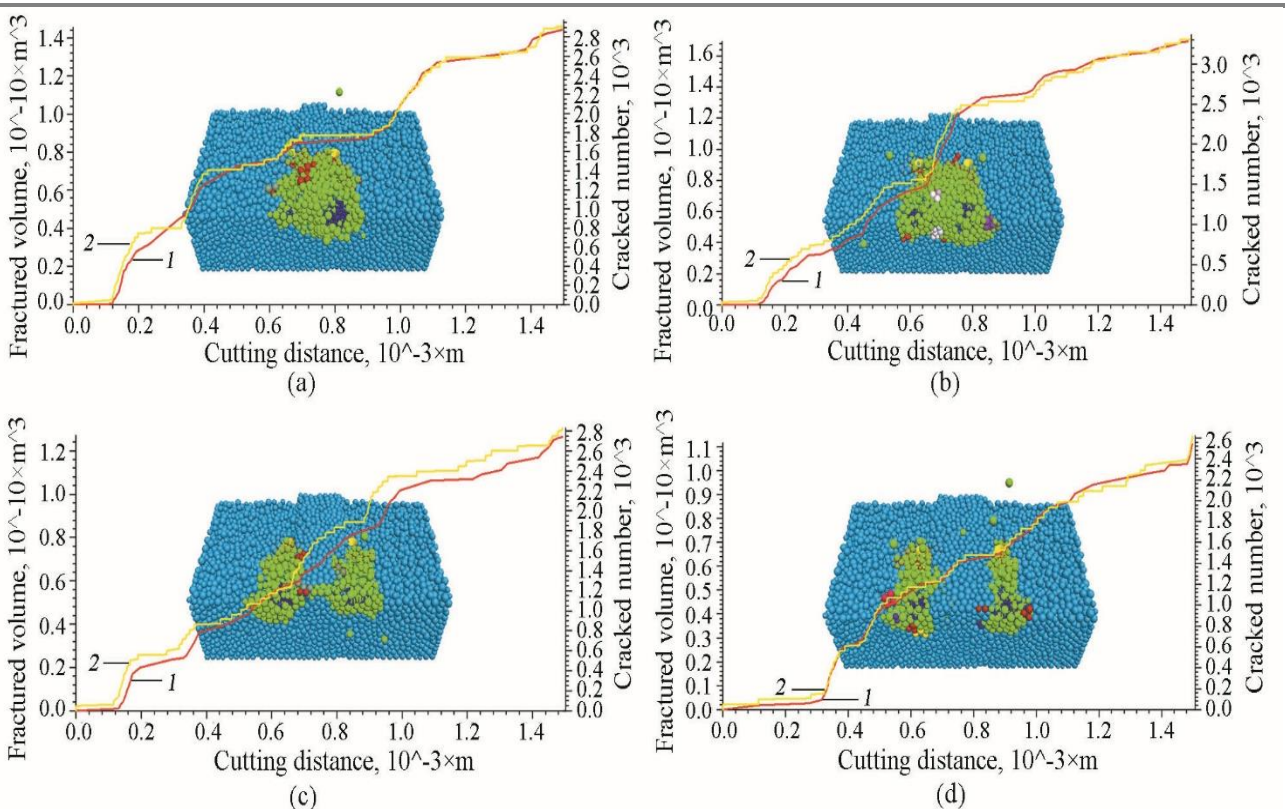


Fig. 5. Fractured volume (1) and number of cracks (2) versus distance between two cutters (diamond granularity 250/180 µm): the distance between two cutters of 1 mm (a), 1.25 mm (b), 1.5 mm (c), 1.75 mm (d).

The simulation results show that the fractured volume and the number of cracks are significantly different with the distance between the two cutters. Table 6 shows the ratio of fractured volume to number of cracks according to the distance between the two cutters. The ratio of the fractured volume to the number of cracks means the fractured volume per unit number of cracks, so it indicates that the larger the value, the larger the particle-size of the fractured cuttings.

Table 6. Ratio of fractured volume to number of cracks according to the distance between two cutters

Distance between two cutters	Fractured volume (×10 <sup>-10</sup> m <sup>3</sup> )	Ratio of fractured volume to number of cracks (×10 <sup>-13</sup> m³/unit)
1mm	1.42	0.493
1.25mm	1.64	0.515
1.5mm	1.22	0.457
1.75mm	1.1	0.423

From Table 6, it can be seen that the appropriate distance between the two cutting for achieving the greatest cutting efficiency is 1.25 mm.

## FIELD DRILLING TESTS

GXY-1 drilling rig was used in the test, and the drilling parameters were set to the weight on bit of 4-5kN, the revolution speed of 654rpm and the flow rate of 20-30L/min. In the drilling tests, ROP and the drilling footage were recorded and the cuttings produced during drilling were collected for analysis. Table 7 shows the drilling test results.



ISSN No. 2321-2705 | DOI: 10.51244/IJRSI | Volume XII Issue X October 2025

Table 7. Drilling test results

Design parameters		Average ROP (m/h)			Drilling footage (m)		
Sub-working layer width	1.25mm	No.1	No.2	Average	No.1	No.2	Average
Matrix hardness	HRC20/25	1.08	1.02	1.05	11.2	10.4	10.8
Diamond granularity	250/180μm						
Diamond concentration	75%						

We conducted a particle-size analysis on the rock cuttings produced during the drilling process. For the particle-size analysis, a LS-POP-6 type particle-size analyzer was used. The particle-size analysis result on the rock cuttings is shown in Fig. 6.

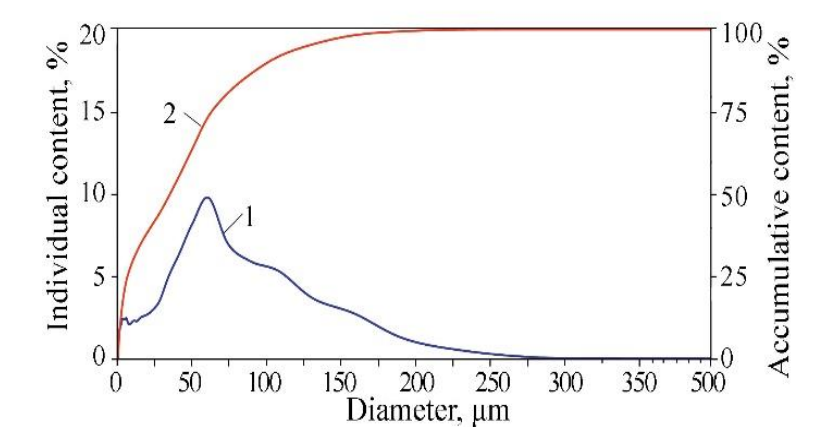


Fig. 6. Particle-size analysis result on the rock cutting produced by SIDB with sub-working layer width of 1.25mm: individual content (1), accumulative content (2).

## RESULTS AND DISCUSSIONS

Through the rock cutting simulation using PFC3D, it has been confirmed that the sub-working layer width has a significant impact on the drilling performance and rock-breaking characteristics of SIDB. From Table 6, it is shown that the fractured volume and the ratio of fractured volume to number of crack is the greatest as  $1.64 \times 10^{-10} \, \mathrm{m}^3$  and  $0.515 \times 10^{-13} \, \mathrm{m}^3$ /unit, respectively when the distance between the two cutters is 1.25 mm. This indicates that the cracks generated at the two cutters are connected together and cause the failure of the rock in the central part simultaneously when the distance between the two cutters is 1.25 mm. When the distance between the two cutters is 1 mm, the cracks generated by the two cutters are connected to each other and the rock in the central part is broken, but the cutting efficiency is less than 1.25 mm. On the other hand, when the distance between the two cutters is greater than 1.5 mm, the ratio of the fractured volume to the number of cracks appears a decreasing trend. This indicates that the cracks generated at each cutter are not connected to each other, and thus do not cause the failure of the rock in the central part. From the simulation results, it can be seen that the appropriate distance between two cutters (appropriate sub-working layer width) is 1.25mm and it seems to significantly improve the drilling performance and the rock-breaking characteristics of SIDB.

Through the field drilling tests, it has been confirmed that the ROP and the drilling footage of SIDB with an appropriate sub-working layer width are greatly improved. From Table 7, it can be seen that the ROP and the drilling footage of SIDB with the sub-working layer width of 1.25 mm are 1.05 m/h and 10.8 m, respectively, and are about 3-5 times larger than those of the conventional bit. Fig. 7 shows the worn SIDB with sub-working layer of 1.25 m.





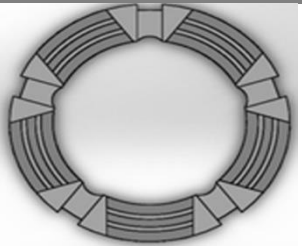


Fig. 7. Worn SIDB with sub-working layer of 1.25mm

The main particle-size of the cuttings produced during the drilling (It means the particle-size of the cuttings that the individual content is more than 5%) ranges from 34.5-108.6 µm (Fig. 6), which is about 8-27 times larger than the particle-size of cuttings (4 µm) [22] produced by a conventional bit. This indicates that the rock-breaking mode of SIDB is clearly transferred from micro-cutting mode to the combination mode of micro-cutting and volumetric-breaking. Also, the bottom area of the main working layer occupies about 72% of the SIDB bottom surface and the drilling specific pressure increases by about 35% from 42 kg/cm² to 57kg/cm². Consequently, the design objective for increasing drilling specific pressure and the particle-size of the cuttings seems to be achieved.

This study allows us to effectively overcome the quartzite formation of Ongjin mining area.

In this study, the impacts of various design parameters such as matrix hardness and diamond concentration and granularity on the drilling performance of SIDB were not considered. Further research is needed to enhance the volumetric-breaking effect of the sandwich structure and improve the drilling performance of SIDB by reasonably designing various design parameters.

This study has proposed a new design approach to effectively overcome the slipping formation.

## CONCLUSIONS

The sub-working layer width has a significant impact on the drilling performance and rock-breaking characteristics of SIDB.

The ROP and the drilling footage of SIDB with the sub-working layer width of 1.25 mm are 1.05 m/h and 10.8 m, respectively, and are about 3-5 times larger than those of the conventional bit.

The rock-breaking mode of SIDB is clearly transferred from micro-cutting mode to the combination mode of micro-cutting and volumetric-breaking and the volumetric-breaking effect appears the most dominantly when the sub-working layer width is 1.25 mm.

The main particle-size of the cuttings produced during the drilling ranges from 34.5-108.6 µm, which enhances the abrasive ability of rock cuttings to the matrix and makes the favorable condition for falling of the blunt diamond grains and protruding of the new diamond grains.

## **ACKNOWLEDGEMENTS**

We thank to all researchers of Faculty of Geoscience and Technology of Kim Chaek University of Technology, who gave us useful assistance and support.

#### COMPLIANCE WITH ETHICAL STANDARDS

## CONFLICT OF INTEREST

The authors have no competing interests to declare that are relevant to the content of this article.





#### **AUTHOR CONTRIBUTIONS**

Il Jin Kim - Investigation, Writing-Original Draft (\*e-mail address: kij911126@star-co.net.kp)

Yong Nam Kim - Project Administration (kyn74628@star-co.net.kp)

Jae Myong Ri - Methodology (ljm6793@star-co.net.kp)

Chol Jong - Conceptualization (jch94123@star-co.net.kp)

Kum Hyok Choe - Software (ckh891224@star-co.net.kp)

#### REFERENCES

- 1. Franca LFP, Mostofi M, Richard T. Interface laws for impregnated diamond tools for a given state of wear. International Journal of Rock Mechanics & Mining Sciences, 2015, vol. 73, pp. 184-193. http://dx.doi.org/10.1016/j.ijrmms.2014.09.010
- 2. Zheng L, Huan HX, Zeng Y, Song SQ, Cheng SL, Zhang CW. A study on the failure mechanism and wear loss of impregnated diamond bits during machining process of armor ceramics. Journal of Mechanical Science and Technology, 2018, vol. 32, no. 1, pp. 261-268. <a href="http://dx.doi.org/10.1007/s12206-017-1226-6">http://dx.doi.org/10.1007/s12206-017-1226-6</a>
- 3. Yang KH, Duan LC. Study on diamond bit for hard and compact rock. Key Engineering Materials, 2004, vol. 259, pp. 46-49. https://doi.org/10.4028/www.scientific.net/KEM.259-260.46
- 4. Wang JL, Zhang SH. Design of impregnated diamond bit based on slipping formaion. Diamond & Abrasives Engineering, 2016, vol. 41, no. 5, pp. 895-900. <a href="https://doi.org/10.3799/dqkx.2016.076">https://doi.org/10.3799/dqkx.2016.076</a>
- 5. Li SB, Xiang Q, Zhang LG. The Wear Mechanisms of Diamond Impregnated Bit Matrix. Applied Mechanics and Materials, 2013, vol. 441, pp. 15-18.
- 6. Mostofi M, Richard T, Franca L, Yalamanchi S. Wear response of impregnated diamond bits. Wear, 2014 vol. 410, pp. 34-42. <a href="https://doi.org/10.1016/j.wear.2018.04.010">https://doi.org/10.1016/j.wear.2018.04.010</a>
- 7. Tan SC, Fang XH, Yang KH, Duan LC. A new composite impregneted diamond bit for extra-hard, compact and nonabrasive rock formation. Int. Journal of Refractory Metals and Hard Materials, 2014, vol. 43, pp. 186-192. <a href="http://dx.doi.org/10.1016/j.ijrmhm.2013.11.001">http://dx.doi.org/10.1016/j.ijrmhm.2013.11.001</a>
- 8. Hu AM. Mechanism of hard abrasive material diamond bit for drilling slipping formation. Low Carbon World, 2014, vol. 4, pp. 130-132.
- 9. Chen Y, Liu DM. Efficient methods applied in slipping strata with diamond bit and its history cases. Superhard Material Engineering, 2006, vol. 18, pp. 16-24.
- 10. Zhang GF, Jiang HD. Development of impregnated diamond bit with primary and secondary abrasives based on matrix weakening theory. International Information and Engineering Technology Association, 2021, vol. 45, no. 3, pp. 259-265. <a href="https://doi.org/10.18280/acsm.450310">https://doi.org/10.18280/acsm.450310</a>
- 11. Liu BX, Cao SQ. Analysis on the slipping form of diamond bit when drilling hard-rock formation and selection of diamond bit. Diamond & Abrasives Engineering, 2011, vol. 31, no. 6, pp. 79-82.
- 12. Li WW, Hu EZ. Research on the technique of manufacturing new diamon bit used for the slipping formation. Superhard Material Engineering, 2008, vol. 20, no. 6, pp. 17-19. http://dx.doi.org/10.1016/j.ijrmhm.2013.11.015
- 13. Sun YS, Wang J, Yang WB. Design of wire-coring impregnated diamond bit for drilling slipping formation. JILIN GEOLOGY, 2012, vol. 31, no. 4, pp. 130-132.
- 14. Qin PG, Jia ZF. Test for improving diamond drilling efficiency in hard-slippery stratum, Engineering construction. 2013, vol. 45, no 4, pp. 42-46.
- 15. Zhao XJ, Li JY, Duan LC, Tan SC, Fang XH. Effect of Fe-based pre-alloyed powder on the microstructure and holding strength of impregnated diamond bit matrix. International Journal of Refractory Metals & Hard Materials, 2019, vol. 79, pp. 115-122.https://doi.org/10.1016/j.ijrmhm.2018.11.015
- 16. Hu HX, Chen W, Deng C, Yang JD. Effect of matrix composition on the performance of Fe-based diamond bits for reinforced concrete structure drilling. International Journal of Refractory Metals and Hard Materials, 2021, vol. 95, pp. 1-10. https://doi.org/10.1016/j.ijrmhm.2020.105419



ISSN No. 2321-2705 | DOI: 10.51244/IJRSI | Volume XII Issue X October 2025

- 17. Martin O, Klaus D, Christos V, Petter E. A bonded-particle model for cemented sand, Computers and Geotechnics, 2013, vol. 49, pp. 299-313. <a href="http://dx.doi.org/10.1016/j.compgeo.2012.09.001">http://dx.doi.org/10.1016/j.compgeo.2012.09.001</a>
- 18. Shi C, Pian JB, Zhang C, Chen X, Zhang YG. Numerical study on rock fracturing with pulsed pressure in hard rocks with a pipe-domain seepage model, Simulation Modelling Practice and Theory, 2024, vol. 130, pp. 1-16. <a href="https://doi.org/10.1016/j.simpat.2023.102860">https://doi.org/10.1016/j.simpat.2023.102860</a>
- 19. Lv YX, Li HB, Zhu XH, Tang LP. Bonded-cluster simulation of rock-cutting using PFC2D, Cluster comput, 2017, vol. 20, pp. 1289-1301. <a href="http://dx.doi.org/10.1007/s10586-017-0808-5">http://dx.doi.org/10.1007/s10586-017-0808-5</a>
- 20. Jia ML, Cai JP, Ouyang ZY, Shen LN, Wu HX, Li C. Design and application of diamond bit to drilling hard rock in deep borehole. Procedia Engineering, 2014, vol. 73, pp. 134-142. https://doi.org/10.1016/j.proeng.2014.06.181
- 21. Potyondy DO, Cundall PA. A bonded-particle model for rock, International Journal of Rock Mechanics & Mining Sciences, 2004, vol. 41, no, 8, pp. 1329-1364. http://dx.doi.org/10.1016/j.ijrmms.2004.09.011
- 22. Wu, J.J., Zhang, S.H., Liu, L.L., Qu, F.L., Zhou, H., and Su, Z., Rock breaking characteristics of a 3D printing grid-matrix impregnated diamond bit, International Journal of Refractory Metals & Hard Materials, 2020, vol. 89, pp. 1-9. https://doi.org/10.1016/j.ijrmhm.2020.105212